SIMULATION OF THREE-DIMENSIONAL LOSS-OF-REGULATION TRANSIENTS IN ACR – 1000 REACTORS

J. Hu§, I. Martchouk, R. Robinson, M. Ovanes, A. Buijs

Atomic Energy of Canada Limited, Mississauga, Ontario, Canada

ABSTRACT

The ACR-1000 reactor regulating system (RRS) provides reactivity control to keep the reactor power at a specified level and to compensate for local changes in reactivity that occur due to effects such as refuelling and fuel burnup. In safety analysis a loss of regulation (LOR) accident is postulated where the overall core reactivity increases linearly, due to a malfunction of the RRS. This causes a power excursion which is terminated by either of the two shutdown safety systems for the ACR. The LOR trip coverage assessment required for the two shutdown systems is traditionally performed with a point kinetics model to predict the bulk power increase following a postulated LOR for a range of assumed reactivity rates that conservatively bound the expected possible reactivity rates for device movement due to malfunctions in RRS. To confirm the validity of these simulations and the conservative margins in this type of analysis a more detailed analysis has been performed using the three-dimensional (3D) kinetics module in the RFSP-IST computer code coupled with the CATHENA thermalhydraulic code. In this paper, the modelling and methodology of the 3D loss of reactivity control analysis are discussed and some limited results are presented.

I. INTRODUCTION

In an ACR-1000®* reactor, the power generated in the fuel at any location in the reactor core depends upon the neutron flux shape and the overall reactor power. Changes in both of these occur during normal operation. The rate of change of the neutron flux is a function of the effective reactivity. Control of reactivity is therefore required to keep the reactor power at the specified level and to compensate for local changes in reactivity that occur due to effects such as refuelling and fuel burnup. Spatial control of reactivity is required to keep the reactor flux shape close to nominal to avoid local power peaking and thus maximize the power produced while not exceeding power limits.

The RRS is designed to perform these functions. It is composed of input sensors (such as ion chambers, fission chambers, in-core flux detectors), control logic, reactivity control devices (zone controllers, mechanical control absorbers), hardware interlocks, and a number of display devices. Reactor regulating system control is accomplished by computer programs which process the inputs and drive the appropriate reactivity control and display devices.

An LOR is an unlikely occurrence in an ACR-1000 reactor. The RRS is designed to have a high degree of reliability and availability. Two independent and identical computers will be used to control the reactor power level and spatial distribution. All functions essential to the reactor operation are incorporated in both computers, one being in control while the other is in backup mode. Most potential

§ Corresponding author, huj@aecl.ca

* Advanced CANDU® Reactor, ACR® and ACR-1000® are registered trademarks of AECL.

failures of the regulating programs result in a “fail-safe” condition, and the reactor automatically shuts down.

The objective of LOR analysis is to demonstrate that each shutdown system can prevent fuel centre line melting and fuel sheath damage, and ensure the heat transport system (HTS) pressure stays within the appropriate limits following a postulated LOR accident. If a fault occurs in the reactor regulating system and leads to an increase in reactivity, the setback or stepback functions would likely intervene and reduce power. However, these are assumed to be unavailable for the purpose of this study.

In this paper, the modelling and methodology of the LOR simulation are discussed. Also presented are results from coupled RFSP-IST and CATHENA dynamic simulations of a fast LOR transient event.

II. REACTOR DESCRIPTION

The ACR-1000 is an evolutionary design of the CANDU reactor characterized by the traditional CANDU fuel channel design, but using low enriched fuel (LEU), light water (H_2O) coolant and heavy water (D_2O) moderator. The core is designed to produce 1150 MW(e) of electrical power. The core has 520 fuel channels arranged in a square array with a lattice pitch of 24.0 cm. Each channel has 12 fuel bundles, and each bundle has 42 fuel elements arranged in three concentric rings around a larger, neutron-absorbing centre element that reduces the coolant void reactivity. To suppress the initial reactivity of the fuel bundles, a small amount of burnable poison, 1 gram per bundle, is included and uniformly distributed in all fresh fuel elements. The ACR-1000 reference equilibrium core fuel load will contain fuel with uniform enriched fuel of 2.4 wt% ^{235}U using a bi-directional 2-bundle shift refuelling sequence.

The main reactor physics design parameters are summarized below in Table 1.

Table 1 ACR 1000 Physics Design Parameters

Parameter	Unit	ACR-1000 Reactor Core
Number of Fuel Channels		520
Number of Bundles per Channel		12
Reflector Average Thickness	cm	60
Core Length	cm	594.36
Calandria Shell Inner Diameter	cm	744
Total Fission Power	MW	3321
Reactor Thermal Power Output	MW	3200
Gross Electrical Power Output	MW	1150
Radial Form Factor[**]		0.94
Fuel Type	wt %	2.4
Fuelling Scheme		2 Bundle Shift
Core-Average Discharge Fuel Burnup	MWd/kgU	20

The ACR-1000 reactors incorporate two passive, fast acting, and separate shutdown systems called SDS1 and SDS2, which are physically and functionally independent of each other. SDS1 consists of mechanical shutoff rods that drop by spring assisted gravity into the core when a trip signal de-

[**] Average channel power divided by peak channel power.

energizes the clutches that hold the shutoff rods out of the core. SDS2 injects a concentrated solution of gadolinium nitrate into the low-pressure moderator to quickly render the core sub-critical. The gadolinium nitrate solution is injected into the core by pressurized helium gas.

III. MODELLING

The simulations have been performed with the code CATHENA (Reference [1]), which employs a multiple average-single-channel model, coupled with an RFSP-IST (References [2] and [3]) three-dimensional neutron kinetic model.

III.A. RFSP-IST Model

The neutron power calculation is done using the ACR-1000 RFSP-IST model. The RFSP-IST (Reactor Fuelling Simulation Program, Industry Standard Toolset) is a computer program for core-wide neutronics calculations in CANDU reactors. RFSP-IST is also used in the ACR-1000 core physics design analysis.

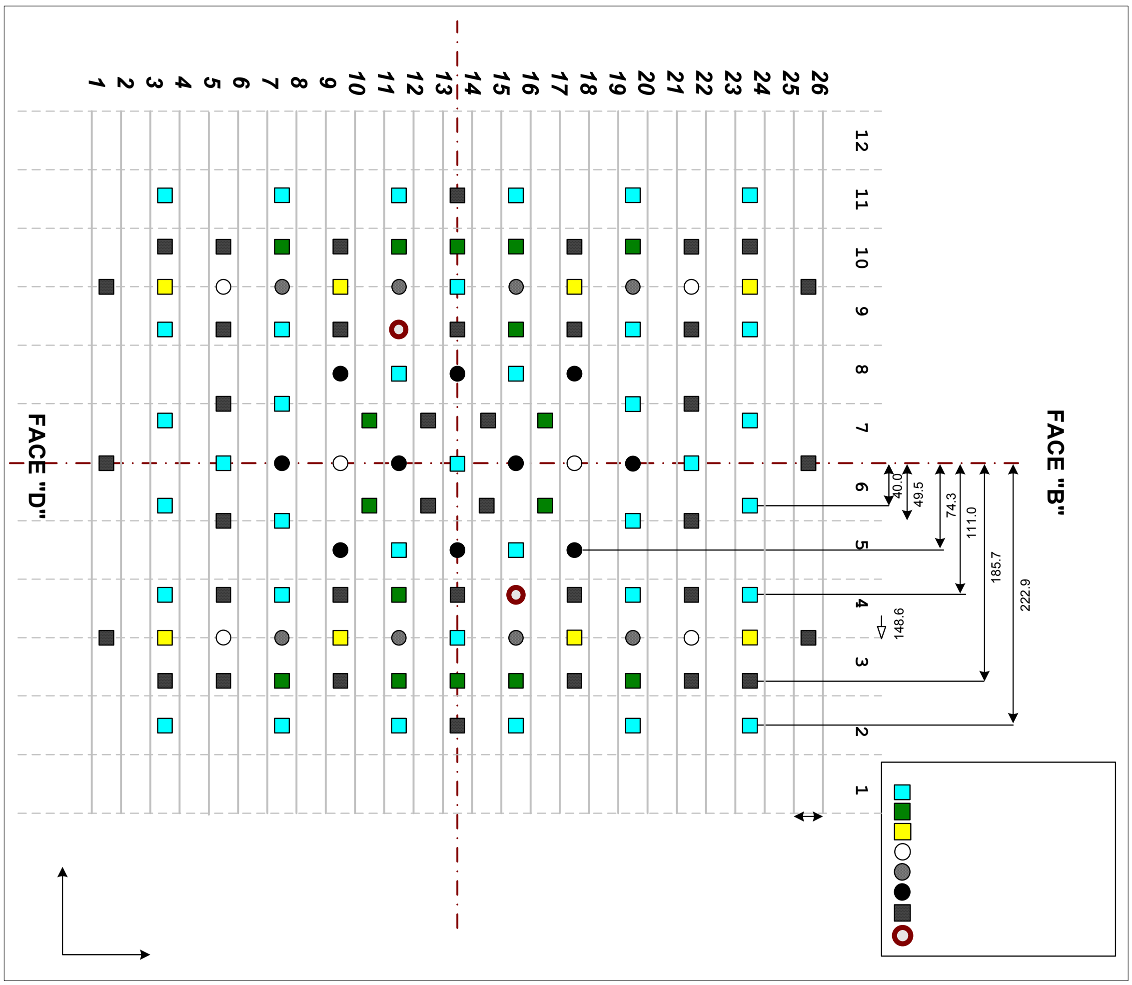

Figure 1 Plan View of Vertical Reactivity Devices and Detector Assemblies for ACR-1000 Reactor

The RFSP-IST core model used in the LOR transient analysis incorporates important information about the fuel bundles, the reflector, the in-core structural materials and the movable reactivity control devices. The core is represented as a grid of lattice cells over the model. In these cells, the nuclear properties are assumed to be homogeneous; the reactivity devices are represented by the corresponding incremental cross sections to be overlaid on the cell fuel properties as well as in the reflector region if applicable. The basis for the core modelling data applicable to the RFSP-IST model used in the present report is given in Table 1.

Figure 1 is a plan view of the ACR-1000 reactivity mechanisms deck. All reactivity devices shown are modelled in the ACR-1000 RFSP-IST model. The LOR transient starts with the withdrawal of the in-core black and grey zone control rods (ZCR) due to a control fault and ends up with the full insertion of safety shutoff rods (SOR) following a Shutdown System one (SDS1) trip. Two independent networks of regional overpower protection (ROP) system detectors, one on each shutdown system, are modelled in the core. The signals from these detectors when they exceed predetermined setpoints in the LOR accident actuate the shutdown systems. Also included in the RFSP-IST core model are four ion chamber units and four fission chamber units, represented by an array of detectors in the reflector, for the neutron flux detection for the log rate trip on SDS1 and SDS2.

The RFSP-IST *CERBERUS module, based on the Improved Quasi-Static method (Reference [4]), computes the time-dependent neutron flux in three spatial dimensions and two energy groups, taking into account delayed-neutron effects which are very significant in fast transients. The *INTREP module calculates fluxes at all detector positions by interpolating in the three-dimensional flux distribution provided by *CERBERUS.

III.B. CATHENA Single Channel Model

The thermal hydraulic transient conditions for the fuel and coolant in the reactor core are provided by the CATHENA (CATHENA MOD-3.5d rev 2) single channel model, which solves a one-dimensional homogeneous two-phase fluid mass, momentum and energy conservation equations and heat-conduction equations in the fuel channel.

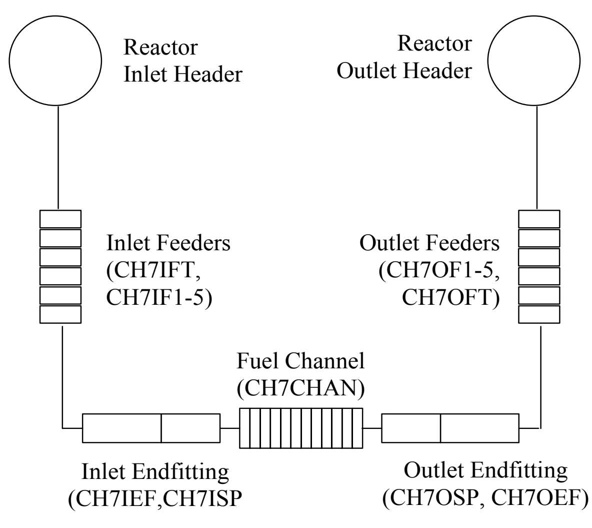

Figure 2 Nodalization of CATHENA Single Channel Model

The components of a single-channel model include inlet and outlet headers (RIH and ROH), feeders, end fittings, pressure tube, and 12 ACR-1000 fuel bundles inside the pressure tube (Figure 2). To analyze the fuel and fuel channel behaviour, each representative channel is divided into twelve characteristic flow regions (axial nodes) corresponding to the twelve fuel bundles within the channel.

The axial nodes are equal in length to the fuel bundles. Each ring of the fuel bundle is simulated as a fuel model, with detailed radiation and alpha-wet/dry models. Pressure tube diametral creeps corresponding to the reactor end-of-life (EOL) condition are taken into account in the thermalhydraulic calculations.

The single channel model represents an individual fuel channel (or a channel group) that defines a thermal hydraulic path from the RIH through the fuel channel to the ROH. Fixed thermalhydraulic boundary conditions in the RIH and ROH are applied for the LOR analysis, which are obtained from the ACR-1000 NUCIRC (Reference [5]) model by using the ACR-1000 time-averaged power distribution and EOL creep.

IV. METHODOLOGY

IV.A. Mechanics of Neutronics-Thermalhydraulics Coupling

LOR transients are simulated by the repeated execution of the neutronics-thermalhydraulics coupling. The RFSP-IST *CERBERUS module is coupled to the CATHENA calculation and receives thermalhydraulic data at the beginning of each simulation. The cycle is repeated at every "flux-shape" time interval (typically 0.25 – 0.5 s), that is, the interval at which *CERBERUS explicitly recalculates the full three-dimensional flux distribution. Thus the neutronics-thermalhydraulic coupling is continuous at all stages of the transient. Note that within each "flux-shape" time interval CATHENA uses its own small time step (e.g. 0.001 s) appropriate to the LOR transients.

The power distribution from *CERBERUS at each "flux-shape" time is fed to CATHENA, which evaluates the coolant densities and fuel and coolant temperatures for the next time when these data are then fed back to *CERBERUS and used in the RFSP-IST calculations. Thus, void and temperature effects on reactivity are taken into account in the core.

The axial power distribution for each channel group is calculated by averaging the bundle powers, provided by the RFSP-IST calculation, over all channels in the thermalhydraulic group. Figure 3 shows the thermalhydraulic groups for all 520 fuel channels. Channels in each group share the same channel power and same axial power distribution while the radial power distribution of a fuel bundle depends on its burnup. The channel grouping is performed according to thermalhydraulic conditions and channel powers predicted by a time-average model of the ACR-1000 equilibrium core.

For the *CERBERUS steady state case 1, the above process is repeated until the relative change in the bundle power distribution between two consecutive RFSP-IST and CATHENA iterations is less than 0.05%.

The LOR transient simulations for this report start from an instantaneous reactor core produced by the RFSP-IST *INSTANTAN module, based on the "patterned-channel-age" model, to represent the variation of the power about the time-averaged power distribution due to refuelling. The "patterned-channel-age" model assumes that irradiation varies linearly with the time during the cycle between refuelling of a specific channel, so that the current value of irradiation is simply a function of the "age" of the channel. Every channel in the core is assigned an age between 0 and 1, where 0 stands for a recently-fuelled channel, and 1 for a channel that is about to be fuelled. A typical channel-age map is presented in Figure 4, where the age is patterned for an array of 7×7 channels, emulating the fuelling sequence and history for a group of 49 channels.

	1	2	3	4	5	6	7	8	9	10	11	12	13	14	15	16	17	18	19	20	21	22	23	24	25	26
A											3	2	1	1	2	3										
B								4	2	3	3	3	3	3	3	3	3	2	4							
C							5	4	6	5	9	10	11	11	10	9	5	6	4	5						
D						7	5	9	9	11	11	12	12	12	12	11	11	9	9	5	7					
E				5	6	8	10	9	11	11	12	12	12	12	12	12	11	11	9	10	8	6	5			
F				7	8	12	10	11	12	12	11	12	12	12	12	11	12	12	11	10	12	8	7			
G			8	8	13	12	12	11	12	12	12	12	12	12	12	12	12	12	11	12	12	13	8	8		
H		5	7	13	13	14	12	12	12	12	12	12	12	12	12	12	12	12	12	12	14	13	13	7	5	
J		5	8	13	14	14	13	12	12	12	13	13	13	13	13	13	12	12	12	13	14	14	13	8	5	
K		6	9	13	14	14	13	13	12	12	13	13	13	13	13	13	12	12	13	13	14	14	13	9	6	
L	7	6	13	14	14	14	13	13	12	12	13	13	12	12	13	13	12	12	13	13	14	14	14	13	6	7
M	7	7	13	14	14	14	13	13	12	12	13	13	11	11	13	13	12	12	13	13	14	14	14	13	7	7
N	7	7	14	14	14	14	13	13	12	12	13	13	11	11	13	13	12	12	13	13	14	14	14	14	7	7
O	7	7	14	14	14	14	13	13	12	12	13	13	11	11	13	13	12	12	13	13	14	14	14	14	7	7
P	7	7	13	14	14	14	13	13	12	12	13	13	11	11	13	13	12	12	13	13	14	14	14	13	7	7
Q	7	6	13	14	14	14	13	13	12	12	13	13	12	12	13	13	12	12	13	13	14	14	14	13	6	7
R		6	9	13	14	14	13	13	12	12	13	13	13	13	13	13	12	12	13	13	14	14	13	9	6	
S		5	8	13	14	14	13	12	12	12	13	13	13	13	13	13	12	12	12	13	14	14	13	8	5	
T		5	7	13	13	14	12	12	12	12	12	12	12	12	12	12	12	12	12	12	14	13	13	7	5	
U			8	8	13	12	12	11	12	12	12	12	12	12	12	12	12	12	11	12	12	13	8	8		
V				7	8	12	10	11	12	12	11	12	12	12	12	11	12	12	11	10	12	8	7			
W				5	6	8	10	9	11	11	12	12	12	12	12	11	11	11	9	10	8	6	5			
X						7	5	9	9	11	11	12	12	12	12	11	11	9	9	5	7					
Y							5	4	6	5	9	10	11	11	10	9	5	6	4	5						
Z								4	2	3	3	3	3	3	3	3	3	2	4							
ZZ											3	2	1	1	2	3										

Figure 3 CATHENA Channel Group Map

	1	2	3	4	5	6	7	8	9	10	11	12	13	14	15	16	17	18	19	20	21	22	23	24	25	26
A											0.16	0.06	0.32	0.36	0.94	0.44										
B								0.44	0.22	0.76	0.54	0.96	0.66	0.58	0.04	0.22	0.88	0.30	0.12							
C							0.84	0.10	0.88	0.02	0.24	0.50	0.28	0.68	0.38	0.76	0.02	0.60	0.18	0.80						
D						0.34	0.26	0.52	0.30	0.60	0.70	0.08	0.82	0.90	0.16	0.54	0.24	0.70	0.92	0.34	0.26					
E				0.08	0.14	0.56	0.72	0.98	0.12	0.18	0.92	0.14	0.40	0.48	0.06	0.96	0.50	0.08	0.14	0.56	0.72	0.98	0.12			
F				0.82	0.40	0.86	0.42	0.64	0.46	0.80	0.34	0.56	0.86	0.78	0.32	0.66	0.28	0.82	0.40	0.86	0.42	0.64	0.46			
G			0.68	0.90	0.48	0.78	0.74	0.20	0.62	0.84	0.26	0.72	0.42	0.74	0.36	0.58	0.68	0.90	0.48	0.78	0.74	0.20	0.62	0.84		
H		0.04	0.38	0.16	0.06	0.32	0.36	0.94	0.44	0.10	0.52	0.98	0.64	0.20	0.94	0.04	0.38	0.16	0.06	0.32	0.36	0.94	0.44	0.10	0.52	
J		0.22	0.76	0.54	0.96	0.66	0.58	0.04	0.22	0.88	0.30	0.12	0.46	0.62	0.44	0.22	0.76	0.54	0.96	0.66	0.58	0.04	0.22	0.88	0.30	
K		0.88	0.02	0.24	0.50	0.28	0.68	0.38	0.76	0.02	0.60	0.18	0.80	0.84	0.10	0.88	0.02	0.24	0.50	0.28	0.68	0.38	0.76	0.02	0.60	
L	0.52	0.30	0.60	0.70	0.08	0.82	0.90	0.16	0.54	0.24	0.70	0.92	0.34	0.26	0.52	0.30	0.60	0.70	0.08	0.82	0.90	0.16	0.54	0.24	0.70	0.92
M	0.98	0.12	0.18	0.92	0.14	0.40	0.48	0.06	0.96	0.50	0.08	0.14	0.56	0.72	0.98	0.12	0.18	0.92	0.14	0.40	0.48	0.06	0.96	0.50	0.08	0.14
N	0.64	0.46	0.80	0.34	0.56	0.86	0.78	0.32	0.66	0.28	0.82	0.40	0.86	0.42	0.64	0.46	0.80	0.34	0.56	0.86	0.78	0.32	0.66	0.28	0.82	0.40
O	0.20	0.62	0.84	0.26	0.72	0.42	0.74	0.36	0.58	0.68	0.90	0.48	0.78	0.74	0.20	0.62	0.84	0.26	0.72	0.42	0.74	0.36	0.58	0.68	0.90	0.48
P	0.94	0.44	0.10	0.52	0.98	0.64	0.20	0.94	0.04	0.38	0.16	0.06	0.32	0.36	0.94	0.44	0.10	0.52	0.98	0.64	0.20	0.94	0.04	0.38	0.16	0.06
Q	0.04	0.22	0.88	0.30	0.12	0.46	0.62	0.44	0.22	0.76	0.54	0.96	0.66	0.58	0.04	0.22	0.88	0.30	0.12	0.46	0.62	0.44	0.22	0.76	0.54	0.96
R		0.76	0.02	0.60	0.18	0.80	0.84	0.10	0.88	0.02	0.24	0.50	0.28	0.68	0.38	0.76	0.02	0.60	0.18	0.80	0.84	0.10	0.88	0.02	0.24	
S		0.54	0.24	0.70	0.92	0.34	0.26	0.52	0.30	0.60	0.70	0.08	0.82	0.90	0.16	0.54	0.24	0.70	0.92	0.34	0.26	0.52	0.30	0.60	0.70	
T		0.96	0.50	0.08	0.14	0.56	0.72	0.98	0.12	0.18	0.92	0.14	0.40	0.48	0.06	0.96	0.50	0.08	0.14	0.56	0.72	0.98	0.12	0.18	0.92	
U			0.28	0.82	0.40	0.86	0.42	0.64	0.46	0.80	0.34	0.56	0.86	0.78	0.32	0.66	0.28	0.82	0.40	0.86	0.42	0.64	0.46	0.80		
V				0.90	0.48	0.78	0.74	0.20	0.62	0.84	0.26	0.72	0.42	0.74	0.36	0.58	0.68	0.90	0.48	0.78	0.74	0.20	0.62			
W				0.16	0.06	0.32	0.36	0.94	0.44	0.10	0.52	0.98	0.64	0.20	0.94	0.04	0.38	0.16	0.06	0.32	0.36	0.94	0.44			
X						0.66	0.58	0.04	0.22	0.88	0.30	0.12	0.46	0.62	0.44	0.22	0.76	0.54	0.96	0.66	0.58					
Y							0.68	0.38	0.76	0.02	0.60	0.18	0.80	0.84	0.10	0.88	0.02	0.24	0.50	0.28						
Z								0.16	0.54	0.24	0.70	0.92	0.34	0.26	0.52	0.30	0.60	0.70	0.08							
ZZ											0.08	0.14	0.56	0.72	0.98	0.12										

Figure 4 A Typical Channel-Age Map

There is no backtracking in the procedure, therefore, the LOR transient simulation has to be run twice. The first time is to calculate the trip time, and the second time the coupled calculation is performed with the shutdown system actuated at the previously calculated trip time.

The output files generated at each step in the LOR transient simulation are automatically renamed and tagged with the *CERBERUS case numbers, allowing a high level of automation in the linking of the codes.

IV.B. Simulation of LOR Transient

As shown in Figure 1, there are 24 zone control units (ZCU) for the ACR-1000 reactor, among which eight units are nominally 50% inserted (called grey ZCU hereafter), 10 units are nominally 100% inserted (black ZCU) and the remaining six units (white ZCU) are normally fully withdrawn. Each unit contains two independently-moveable absorber elements (upper and lower). The grey ZCUs are purely for the RRS while the black ZCUs are part of the RRS and are also used to provide positive reactivity when withdrawn from the core.

In this study the LOR event simulated occurs due to a control fault where all the in-core ZCUs (36 black and grey rods) drive out at the maximum speed from an initial critical core at full power.

IV.C. Actuation Times for Shutdown System

In the early stages of the LOR transients, a *perl* script is run to read-in the readings of in-core ROP detectors and ion/fission chambers and thereby determine the times at which trip setpoints are reached.

There are eight in-core ROP detector systems (four for SDS1 and four for SDS2), four fission chamber units (for SDS1) and four ion chamber units (for SDS2) for the ACR-1000 reactor. They are all included in the RFSP-IST model to calculate actuation times of the shutdown systems.

Each ROP system consists of 20 to 30 self-powered in-core flux detectors, contained within the core in vertical or horizontal tubes known as assemblies. Those flux detector assemblies are located within the relatively cool low-pressure moderator, between and perpendicular to the fuel channels. To ensure physical separation, the SDS1 ROP detectors and shutdown mechanisms are vertically oriented, while the SDS2 detectors and poison injection tubes are horizontal. The ion/fission chamber units are represented by an array of detectors located in the reflector (although, in reality, they are located on the calandia shell wall), providing detector readings for the trip time calculation by checking the log rate of the reactor power increase.

Each detector in the ROP system or ion/fission chamber unit has a preset trip setpoint. If the signal from any detector in a trip channel exceeds the detector’s setpoint, then that trip channel is tripped. Trip by any two out of the four trip channels initiates a reactor shutdown.

IV.D. Flux-Shape Time Interval

A variable flux-shape time Δt was used in this transient. Up to the time of actuation of SDS1, a constant Δt value of 0.25 s was adopted. Following the SDS1 actuation, variable values of Δt were chosen to make the flux-shape calculations coincide with the instant at which the leading edge of the shutoff rods reaches the bottom line of each fuel channel row to avoid non-conservative smearing of the effect of the SORs in the RFSP-IST model. Based on this criterion, values of Δt in the range of 0.05 – 0.10 seconds were used until full shutoff-rod insertion. These small values ensure good convergence in the time behaviour of the *CERBERUS solution. Following shutoff-rod complete insertion, the flux-shape changes are small and larger values of Δt are appropriate.

Within each time interval Δt, the CATHENA calculation uses its own time step of the order to 1 millisecond and assumed a constant reactor core power distribution.

IV.E. Assumptions and Input Data

Following assumptions are made in this LOR analysis:

- The reactor is initially at a steady state at 100% full power (FP). No power tilt is applied. The LOR transient starts from an instantaneous (patterned age) reactor core.
- A uniform pressure tube (PT) creep of 3.29% is applied for the ACR-1000 reactor end-of-life (EOL) core RFSP-IST model while distributed PT creeps are used in the CATHENA model.
- Moderator temperature and density are assumed to be spatially uniform and do not change during the fast LOR transients.
- Speeds of the grey and black ZCUs are constant during the LOR transient. The times for all grey and black ZCUs to move from their fully-inserted positions to their fully-withdrawn positions are assumed to be the same, equal to 60 seconds, even though the rods near the centre of the core are longer than those near the edge of the core.
- The radial power fraction, i.e., the power percentage for the three fuel rings of a fuel bundle, is dependent of the bundle burnup while the power fraction for the central poison pin is kept constant at 0.34%, obtained from MCNP simulation studies on a mid-burnup 2.4% LEU fuel bundle.
- For an LOR event, the effective trip parameters are high neutron power (ROP), high log rate (ion/fission chambers), and heat transport system high pressure (HP). The ROP trip setpoints for SDS1 and SDS2 are set to 115%. High log rate trip setpoints for the ion/fission chambers are set to 11%. No HP trip is credited in the report.
- The trip-chain electronics of the in-core ROP detectors and ion/fission chambers are not simulated. A delay of 150 milliseconds is added to the SDS1 actuation time, instead.
- For a conservative analysis of the SDS1, it is assumed that two shutoff rods are nonoperational in the *CEBERUS calculation. The missing rods are chosen such that the remaining shutoff rods are the least effective.
- The thermalhydraulic boundary conditions for the CATHENA single channel model are assumed to be constant during the fast LOR transient.

IV.F. Computer Codes

The LOR transient analysis has been performed on the AECL Linux cluster. The RFSP-IST executable is of version 3.05; CATHENA executable is of version MOD-3.5d/Revision 2.

V. RESULTS

An LOR transient event is simulated to test the methodology of the RFSP-IST and CATHENA coupling. In this event, all the black ZCUs (nominally 100% in) and grey ZCUs (nominally 50% in) start moving, at a constant rate out of the reactor core at t=0 s when the reactor is operating at full power critical state, as illustrated in Figure 5 where the *y* axis stands for the distance between the ends of the ZCU rods to the calandria wall.

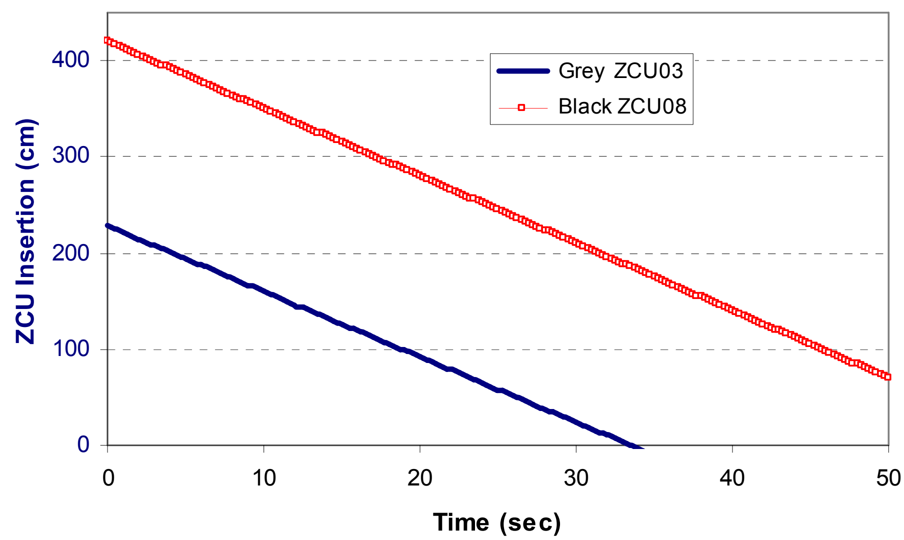

Figure 5 Movement of Black and Grey ZCUs during LOR

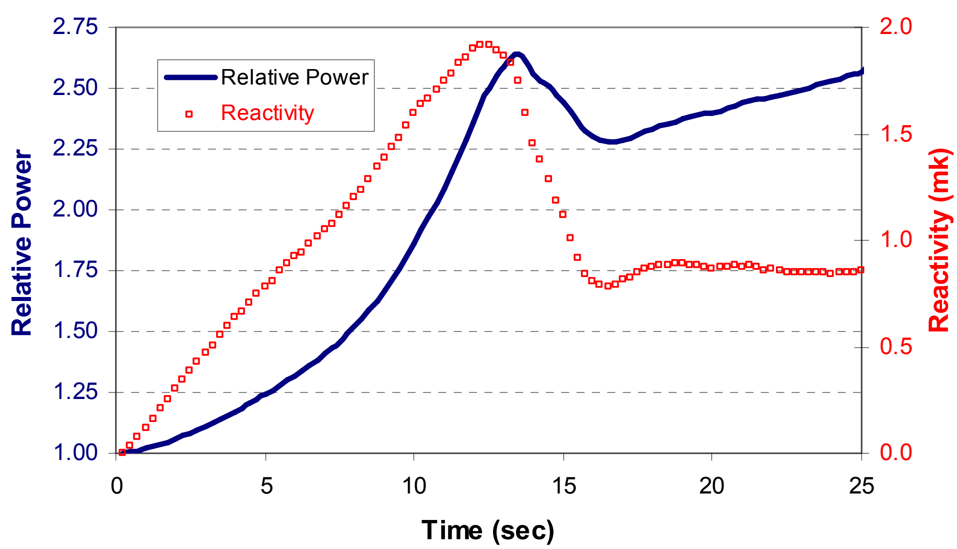

Figure 6 Power transient and reactivity change during LOR without SDS1 trip

The transient simulation is carried out twice. The first time simulation is used to calculate the trip time for SDS1. Figure 6 presents the interplay of the total relative reactor power (denoted by blue histogram) on the reactivity change (denoted by open red squares) during the transient. The reactivity is increasing up to about 12.5 s, at which time it begins to decrease due to the fuel temperature feedback effect plus the contribution from the change in the coolant density, as shown in Figure 7. The total reactor power, however, turns over at around 13.5 s though at this time the reactivity is still positive. This is due to the contribution from the delayed neutrons. Figure 7 also shows the core-averaged coolant density transient (denoted by blue histogram).

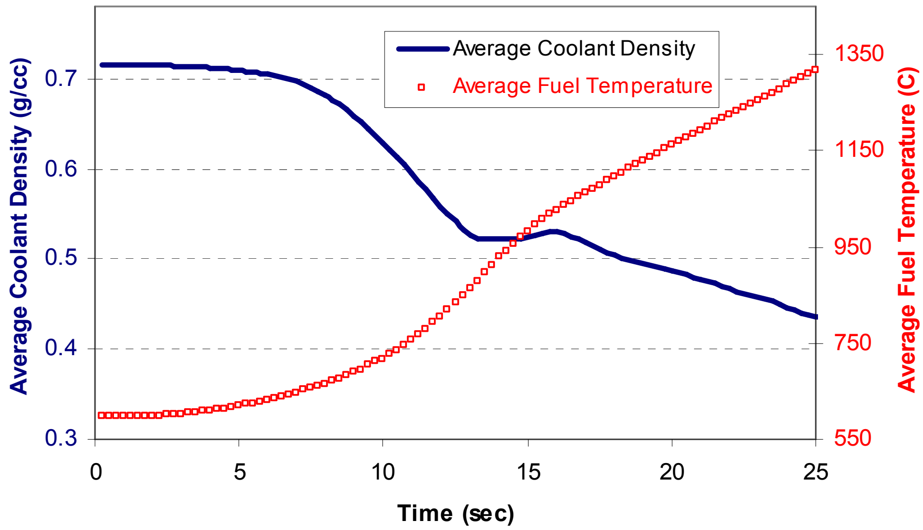

Figure 7 Core average coolant density and fuel temperature during LOR without SDS1 trip

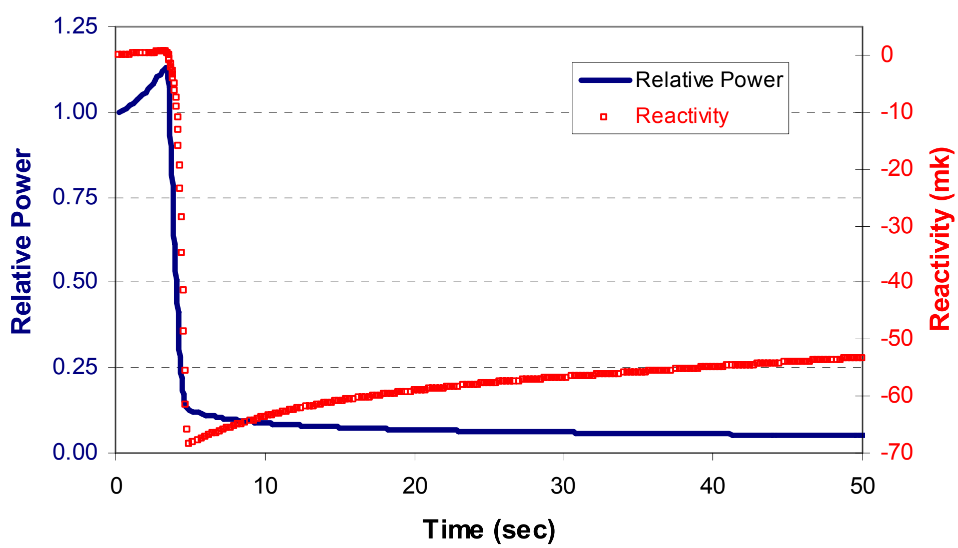

Figure 8 Power transient and reactivity change during LOR with SDS1 trip

The SDS1 actuation time is found to be about 2.67 s due to the ROP high neutron power trip.

The simulation is then performed with the SDS1 trip included. Figure 8 shows the total reactor power transient and reactivity change up to 50 s, illustrating the effect of the SDS1 actuation. No dryout occurs during the whole transient. The core-averaged coolant density and fuel temperature distributions are given in Figure 9. The fuel bundle is gradually cooled down by the coolant after the reactor is shutdown.

To test the validity of the CATHENA single channel model in the fast LOR simulation, another analysis is done with the variable thermalhydraulic boundary conditions which are obtained from a CATHENA-only analysis by using the circuit model. The discrepancy is found to be negligible (less than 0.15%) for the LOR trip case.

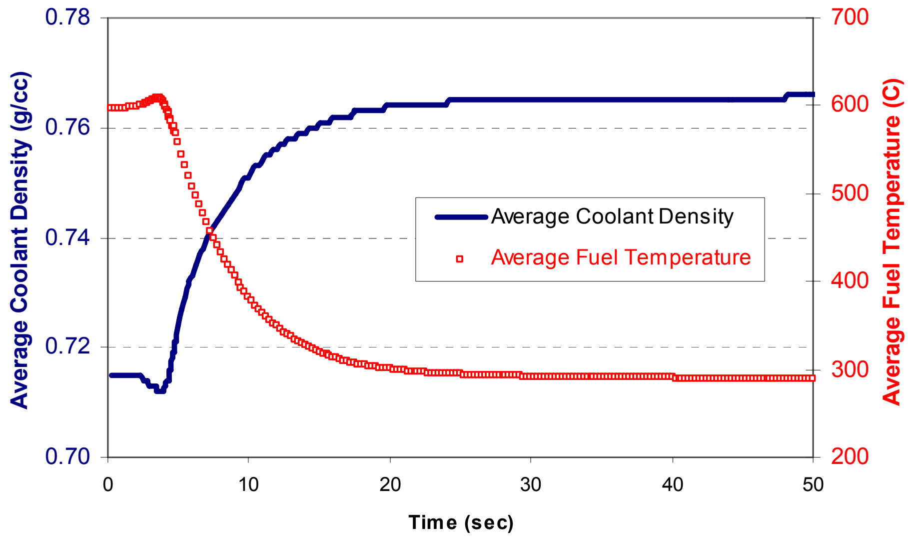

Figure 9 Core average coolant density and fuel temperature during LOR with SDS1 trip

VI. SUMMARY

A package for coupled neutronics-thermalhydraulics analysis of LOR transients has been developed. The methodology and the relevant *perl* scripts have been tested.

Results show that for the 3D LOR transient considered here, where all grey and black ZCU rods drive out at a maximum rate due to a control malfunction, the reactor trips on the ROP high power and the total reactor power is reduced before fuel failure. This result is consistent with the one dimensional analysis with point kinetics model. As such, no unusual effects due to the 3D simulation have been uncovered. Future work will look at 3D LOR simulations for different initiating transients and different starting flux shapes.

VII. REFERENCES

[1] B.N. Hanna, "CATHENA: A Thermalhydraulic Code for CANDU Analysis", J. Nucl. Eng. Design 180: 113-131, 1998.

[2] B. Rouben, "RFSP-IST, The Industry Standard Tool Computer Program for CANDU Reactor Core Design and Analysis", Proceeding of the 13th Pacific Basin Nuclear Conference, Shenzhen, China, October 21-25 (2002).

[3] W. Shen, "Development of a Multicell Methodology to Account for Heterogeneous Core Effects in the Core-Analysis Diffusion Code", American Nuclear Society's Topical Meeting on Reactor Physics - PHYSOR-2006, Vancouver, September 10-14, 2006.

[4] D.A. Meneley, K.O. Ott, E.S. Wiener, "Fast-Reactor Kinetics – the QX1 Code", ANL-7769, Argonne National Laboratory, Argonne, IL, USA (1971).

[5] D.J. Wallace and W. Hartmann, "A Review of NUCIRC Development in Support of CANDU Plant Aging Assessments", Proceedings of the CNS 6th International Conference on Simulation Methods in Nuclear Engineering, Montreal, Quebec, Canada, Oct. 2004.